PAPER

NJC
www.rsc.org/njc

Synthesis and time-resolved fluorimetric application of a europium chelate-based phosphorescence probe specific for singlet oxygen

Bo Song, Guilan Wang, Mingqian Tan and Jingli Yuan*

Department of Analytical Chemistry, Dalian Institute of Chemical Physics, Chinese Academy of Sciences, Graduate School of the Chinese Academy of Sciences, Dalian, 116023, P. R. China. E-mail: jingliyuan@yahoo.com.cn; Fax: +86-411-84379660; Tel: +86-411-84379660

Received (in Montpellier, France) 26th July 2005, Accepted 17th August 2005
First published as an Advance Article on the web 5th September 2005

A new europium chelate, [4′-(9-anthryl)-2,2′:6′,2″-terpyridine-6,6″-diyl]bis(methylenenitrilo) tetrakis(acetate)-Eu^{3+} (ATTA-Eu^{3+}), has been designed and synthesized as a highly sensitive and selective time-resolved phosphorescence probe for singlet oxygen ($^1O_2$). The probe can specifically react with $^1O_2$ to yield its endoperoxide (EP-ATTA-Eu^{3+}) with a great increase of the luminescence quantum yield and a long phosphorescence lifetime of 1.21 ms, which renders the probe favorable to be used for highly sensitive time-resolved luminescence detection of $^1O_2$. The new phosphorescence probe is highly water soluble with a large stability constant of $\sim 10^{20}$ and a wide available pH range at pH > 3. Upon reactions with some reactive oxygen species including hydrogen peroxide, superoxide, hydroxyl radical and $^1O_2$, the probe shows high specificity for $^1O_2$. The probe was used for quantitative detection of $^1O_2$ generated from a MoO_4^{2-}–H_2O_2 system to give a detection limit of 2.8 nM. Furthermore, the good applicability of the probe was demonstrated by the real-time monitoring of the kinetic process of $^1O_2$ generation in a horseradish peroxidase (HRP) catalyzed oxidation system of indole-3-acetic acid (IAA) in a weakly acidic buffer and in a photosensitization system of 5,10,15,20-tetrakis(*N*-methyl-4-pyridyl)-21*H*,23*H*-porphine (TMPyP) in a neutral buffer.

Introduction

The lowest excited electronic state of molecular oxygen, singlet oxygen ($^1O_2$), is an important intermediate in many chemical and biological processes. It has aroused much interest as a biological oxidant and its role in photobiological processes has been well documented.[1] In addition, there is overwhelming evidence that excited state species produced by biochemical reactions in cells and tissues exposed to oxidative stress may subsequently react with ground-state oxygen to yield $^1O_2$ as in photosensitization.[2] Singlet oxygen has a unique reactivity that can result, for example, in polymer degradation[3] or the death of biological cells which is exploited in photodynamic therapy,[4] and furthermore, it likely plays an important role in the cell signalling cascade and in the induction of gene expression.[5] However, some results are still controversial, mainly because of the lack of a reliable detection method for $^1O_2$.[6]

Monitoring the direct emission of $^1O_2$ at 1270 nm is a specific and non-invasive method, but this method suffers from weak signal, and quantitative detection of very small amount of $^1O_2$, as low as 100 nM, is currently not possible in any medium.[6,7] Chemical trapping by spectroscopic probes is also found to be specific and more sensitive than the detection of the 1270 nm luminescence. The most widely used $^1O_2$ trap is 9,10-diphenylanthracene (DPA), which can specifically react with $^1O_2$ to form a thermostable endoperoxide at a rate of $k = 1.3 \times 10^6$ M^{-1} s^{-1}, with the decrease in absorbance at 335 nm as a signal of $^1O_2$ production.[8] However, this method is also less sensitive because the detection is based on the measurement of absorbance. To improve the detection sensitivity, fluorescent probes were developed by incorporating the reactive anthracene moiety into a xanthene ring.[9] These probes can react with $^1O_2$ to yield the corresponding endoperoxides giving sensitive fluorescence responses. The limitations of these probes are that they cannot be used at lower pH, where the endoperoxides are non-fluorescent, and they are obviously limited to steady-state investigations.[6,9] Recently, Li *et al.* developed a chemiluminescence probe for $^1O_2$ by conjugating an electron-rich tetrathiafulvalene unit with a reactive luminophore of anthracene.[10] This probe exhibits strong chemiluminescence response and high selectivity for $^1O_2$ with a detection limit of 76 nM. The main drawback of this probe is its lower water solubility: a buffer containing 50% tetrahydrofuran (THF) is necessary to dissolve the probe, which makes it not very suitable for biosystems.

Time-resolved fluorimetry using lanthanide chelates as luminescence probes has been widely used in highly sensitive fluoroimmunoassay and DNA hybridization assay.[11] The most important advantage of this technique is that the method can effectively eliminate the short-lived background noise from the biological samples and the optical components.

In a preliminary communication,[12] we described that a Eu^{3+} chelate, [4'-(9-anthryl)-2,2′:6′,2″-terpyridine-6,6″diyl]bis(methylenenitrilo)tetrakis(acetate)-Eu^{3+} (ATTA-Eu^{3+}) can be used as an efficient phosphorescence probe for $^1O_2$. Herein we report the synthesis and time-resolved fluorimetric application of ATTA-Eu^{3+} as a highly selective and sensitive luminescence probe for $^1O_2$ assay. This Eu^{3+} chelate is almost non-luminescent, and can specifically react with $^1O_2$ to form a strongly luminescent endoperoxide (EP-ATTA-Eu^{3+}, Scheme 1) with a long phosphorescence lifetime, which can be used for time-resolved luminescence measurement. A strong luminescence response was found upon the reaction of ATTA-Eu^{3+} with $^1O_2$ only, but not with other reactive oxygen species such as hydrogen peroxide, superoxide, and hydroxyl radical, showing an extremely high selectivity for $^1O_2$. The probe's applicability for $^1O_2$ detection has been demonstrated by quantitative detection of $^1O_2$ generated from a MoO_4^{2-}–H_2O_2 system in a

DOI: 10.1039/b510611g

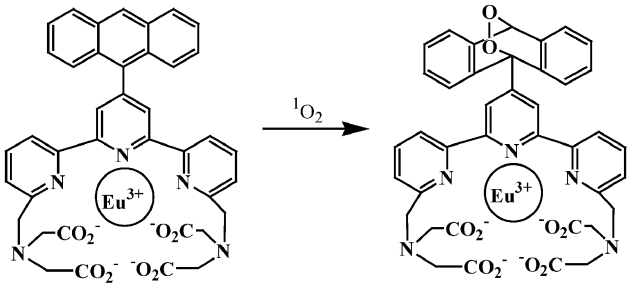

Scheme 1 Reaction of ATTA-Eu^{3+} with $^1O_2$.

weakly basic buffer, the assay of $^1O_2$ formation by the irradiation of a photosensitizer in a neutral buffer, and real-time monitoring of $^1O_2$ generation during the horseradish peroxidase (HRP)-catalyzed oxidation of indole-3-acetic acid (IAA) in a weakly acidic buffer.

Results and discussion

Design and synthesis of the europium chelate-based phosphorescence probe for $^1O_2$

The time-resolved fluorimetric probe specific for $^1O_2$ was designed by incorporating the strong fluorophore (2,2′: 6′, 2″-terpyridine-6,6″-diyl)bis(methylenenitrilo)tetrakis(acetate)-Eu^{3+} (TTA-Eu^{3+}) into a reactive moiety of anthracene specific for $^1O_2$. We chose TTA-Eu^{3+} as a fluorophore since it has higher luminescence quantum yield and solubility in aqueous buffers.[13] It has been well-known that the anthracene skeleton can specifically trap $^1O_2$ to form endoperoxide[8–10] and efficiently quench the fluorescence of the fluorophore conjugated with it.[9,14] Before reacting with $^1O_2$, the Eu^{3+} chelate is almost non-luminescent due to the strong luminescence quenching effect of 9-anthryl moiety, which is favorable to afford a low background signal. After the chelate is specifically reacted with $^1O_2$ to yield its endoperoxide (EP-ATTA-Eu^{3+}), the chelate becomes strongly luminescent with a long phosphorescence lifetime, which can be easily used for highly sensitive time-resolved luminescence measurement.

The ligand ATTA was synthesized following the eight-step reaction as shown in Scheme 2. The corresponding endoperoxide of its Eu^{3+} chelate was synthesized by reacting ATTA-Eu^{3+} with chemically generated $^1O_2$ (MoO_4^{2-}–H_2O_2).[15] The production of EP-ATTA-Eu^{3+} was confirmed by its ESI mass spectrum. When EP-ATTA-Eu^{3+} was challenged with a five-fold excess of ethylenediamine tetraacetic acid, a conditional stability constant was measured to be $\sim 10^{20}$ by using Verhoeven's method.[16] Moreover, no decrease of the phosphorescence intensity of EP-ATTA-Eu^{3+} was observed after several days at room temperature. Using the luminescence lifetimes of ATTA-Eu^{3+} and EP-ATTA-Eu^{3+} in H_2O and D_2O buffers, the average number (q) of water molecules in the first coordination sphere of Eu^{3+} ion was calculated from the equation

$$q = 1.2\,(1/\tau_{H_2O} - 1/\tau_{D_2O} - 0.25)$$

to be 0.05 and 0.04, respectively.[17] These results indicate that the probe has a high kinetic and thermodynamic stability, and the increase of the probe's phosphorescence intensity is not caused by the decrease of the number of the coordinated water molecules.[18]

Phosphorescence properties of the chelate

The phosphorescence properties of ATTA-Eu^{3+} and EP-ATTA-Eu^{3+} are listed in Table 1. The excitation and emission maximum wavelengths ($\lambda_{ex,max}$, $\lambda_{em,max}$) are not changed, which is similar to Nagano's probe,[9] and molar absorption coefficients (ε) and phosphorescence lifetimes (τ) are changed slightly from ATTA-Eu^{3+} to EP-ATTA-Eu^{3+}. As expected, ATTA-Eu^{3+} itself is almost non-luminescent with a very low luminescence quantum yield, and EP-ATTA-Eu^{3+} is strongly luminescent, since the luminescence quantum yield (ϕ) of EP-ATTA-Eu^{3+} is 17 times higher than that of ATTA-Eu^{3+}. As shown in Fig. 1A, ATTA-Eu^{3+} and EP-ATTA-Eu^{3+} show excitation maximum wavelengths at 289 nm and 335 nm, and several discrete emission bands between 580 and 710 nm corresponding to the $^5D_0 \rightarrow {}^7F_J$ (J = 0–4) transitions of Eu^{3+}. This emission feature indicates that the emission of the probe can be monitored at several discrete points between 580 and 710 nm. The absorption spectra of ATTA-Eu^{3+}

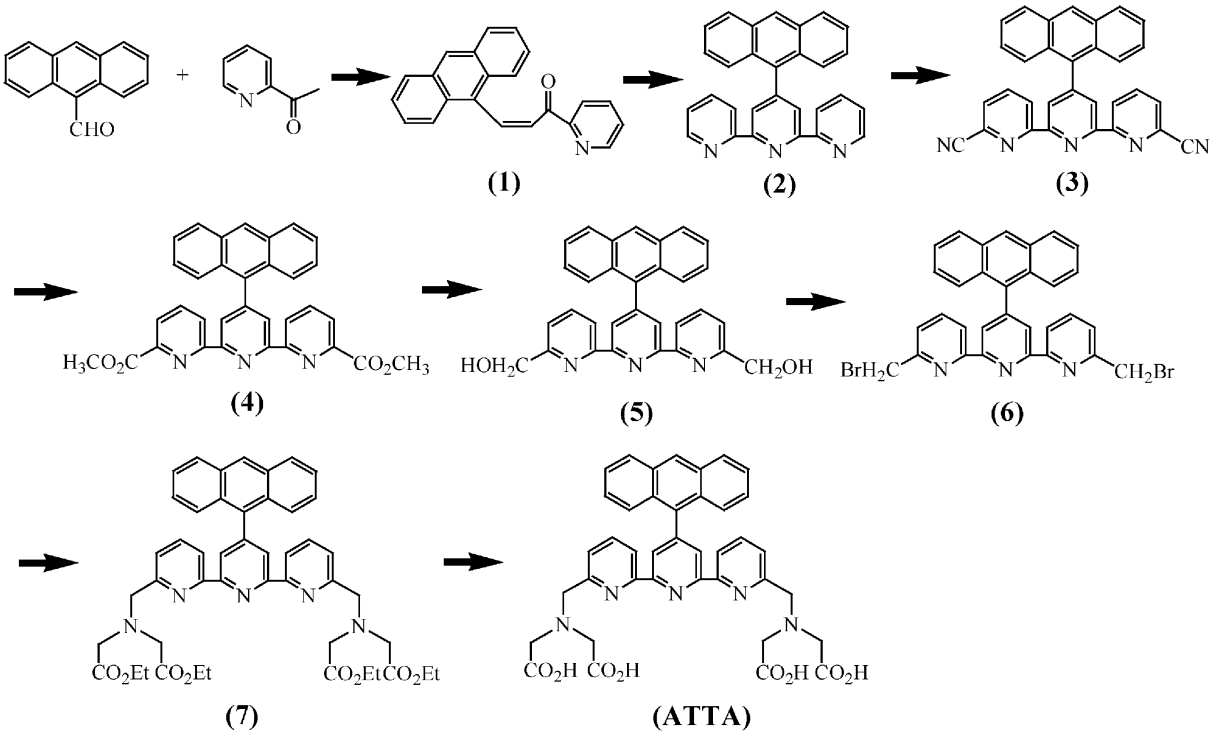

Scheme 2 Synthesis of ATTA.

Table 1 Phosphorescence properties of ATTA-Eu^{3+} and EP-ATTA-Eu^{3+} [a]

	$\lambda_{ex,\ max}$/nm	$\lambda_{em,\ max}$/nm	ϕ (%)	$\varepsilon_{335\ nm}$/cm^{-1} M^{-1}	τ/μs[b]
ATTA-Eu^{3+}	289, 335	615	0.58	17 200	989
EP-ATTA-Eu^{3+}	289, 335	615	10.0	14 500	1209

[a] All data were obtained in 0.05 M borate buffer of pH 9.1. [b] In H_2O and D_2O solutions, phosphorescence lifetimes of ATTA-Eu^{3+} are 1.10 and 1.64 ms, and those of EP-ATTA-Eu^{3+} are 1.37 and 2.23 ms, respectively.

and EP-ATTA-Eu^{3+} are shown in Fig. 1B. The two absorption bands between 350–400 nm caused by the absorption of the probe's 9-anthryl moiety disappeared after the formation of EP-ATTA-Eu^{3+}, which also indicates that the 9-anthryl group in the probe is a functional group to specifically trap $^1O_2$.

The effects of pH on the phosphorescence intensity and lifetime of EP-ATTA-Eu^{3+} were measured by using a solution of 1.0 μM EP-ATTA-Eu^{3+} in 0.05 M Tris-HCl buffers with different pHs (from 2.0–10.2). As shown in Fig. 2, in contrast to the rapid decrease of fluorescence intensity of fluorescein-based probes at pH < 7,[9] the phosphorescence intensity of EP-ATTA-Eu^{3+} is stable at pH > 3 (it must be considered that the chelate itself is not stable in a buffer of pH < 3). This result indicates that ATTA-Eu^{3+} is useful as a phosphorescence probe for $^1O_2$ detection in weakly acidic, neutral and basic buffers.

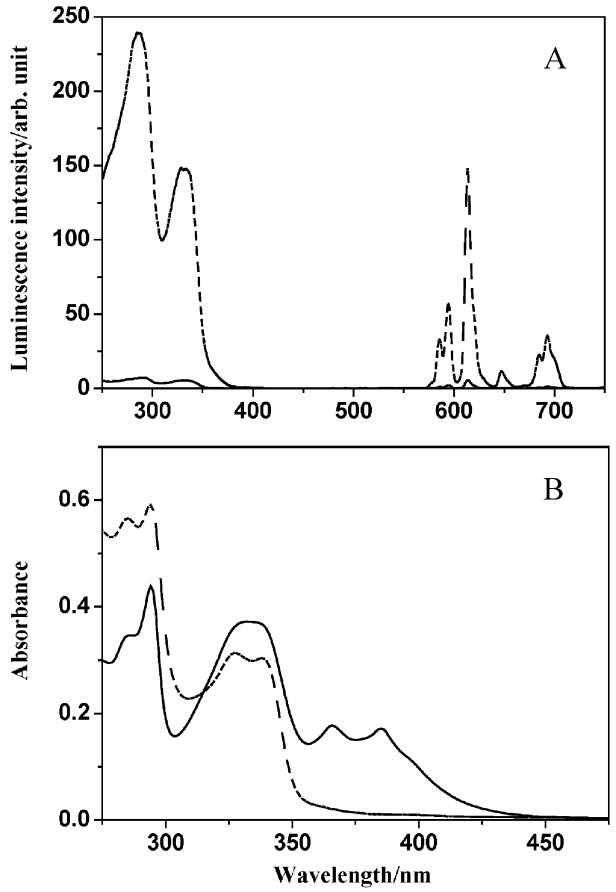

Fig. 1 (A) Time-resolved excitation and emission spectra of ATTA-Eu^{3+} (1.0 μM, solid line) and EP-ATTA-Eu^{3+} (1.0 μM, dashed line) in a 0.05 M borate buffer of pH 9.1. The conditions of delay time, 0.2 ms; gate time, 0.4 ms; cycle time, 20 ms; excitation slit, 10 nm; and emission slit, 5 nm were used for the measurements. Excitation spectra were recorded with $\lambda_{em} = 615$ nm and emission spectra with $\lambda_{ex} = 335$ nm. (B) Absorption spectra of ATTA-Eu^{3+} (20 μM, solid line) and EP-ATTA-Eu^{3+} (20 μM, dashed line) in a 0.05 M borate buffer of pH 9.1.

Reactions of the probe with reactive oxygen species

The reactions of ATTA-Eu^{3+} with different reactive oxygen species (H_2O_2, $^{\bullet}OH$, $O_2^{-\bullet}$, and $^1O_2$) were investigated to examine its selectivity in the same buffer. As shown in Fig. 3, the phosphorescence intensities of the products of ATTA-Eu^{3+} reacted with H_2O_2, $^{\bullet}OH$ and $O_2^{-\bullet}$ did not give noticeable change, whereas a remarkable increase was observed after the chelate was reacted with $^1O_2$. Since the phosphorescence intensities, excitation and emission spectra of the mixtures of ATTA-Eu^{3+} with H_2O_2, $^{\bullet}OH$ or $O_2^{-\bullet}$ are not greatly changed, it can be considered that the probe does not react with these species. When azide (1.0 mM), a quencher of $^1O_2$,[19] was added to a MoO_4^{2-} (10 mM)–H_2O_2 (20 mM)–ATTA-Eu^{3+} (0.1 mM) system, a change in the probe's phosphorescence intensity was not observed. These results indicate that the probe ATTA-Eu^{3+} is highly specific for $^1O_2$, which can be attributed to the specific reactivity of anthracene unit toward $^1O_2$.[8–10]

Detection of $^1O_2$ in aqueous media

Since $^1O_2$ can be quantitatively generated in a basic aqueous buffer through H_2O_2 disproportionation catalyzed by molybdate ions,[15] the MoO_4^{2-}–H_2O_2 system was used as a chemical source of $^1O_2$ to investigate the reaction of ATTA-Eu^{3+} with $^1O_2$. The reaction was performed in 0.1 M carbonate buffer of pH 10.5. Fig. 4 shows the time-resolved excitation (A) and emission (B) spectra of ATTA-Eu^{3+} reacted with different concentrations of $^1O_2$, which reveals the effect of the formation of EP-ATTA-Eu^{3+} on the phosphorescence intensity of the Eu^{3+} chelate. The phosphorescence intensity is increased with the increase of $^1O_2$ concentration in a dose-dependent manner, and a good linearity between the phosphorescence intensity and the $^1O_2$ concentration was obtained (Fig. 5). The detection limit for $^1O_2$, calculated as the concentration corresponding to three standard deviations of the background signal, is 2.8 nM, which is ~28 times lower than that of the chemiluminescence method,[10] and indicates that the $^1O_2$ detection using the new probe is highly sensitive.

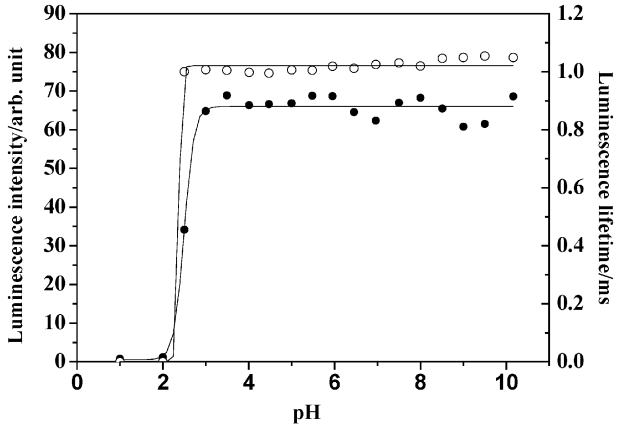

Fig. 2 Influences of pH on the luminescence intensity (●) and lifetime (○) of EP-ATTA-Eu^{3+} (1.0 μM in 0.05 M Tris-HCl buffer). The luminescence intensity was measured with a time-resolved mode with the conditions of excitation wavelength, 335 nm; emission wavelength, 615 nm; delay time, 0.2 ms; gate time 0.4 ms; cycle time, 20 ms; excitation slit, 10 nm; and emission slit, 5 nm.

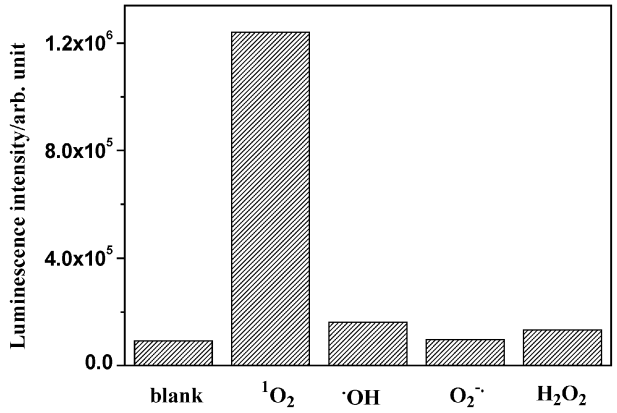

Fig. 3 Luminescence intensities of the products of ATTA-Eu^{3+} (100 nM) reacted with different reactive oxygen species. $^1O_2$: 10 μM H_2O_2 + 10 mM Na_2MoO_4; $^{\bullet}OH$: 10 μM H_2O_2 + 10 μM ferrous ammonium sulfate; $O_2^{-\bullet}$: 10 μM KO_2; H_2O_2: 10 μM H_2O_2.

Singlet oxygen produced by the irradiation of a photosensitizer in a neutral buffer was also detected by using ATTA-Eu^{3+} as a probe. A water-soluble cationic porphyrin, 5,10,15,20-tetrakis(*N*-methyl-4-pyridyl)-21*H*,23*H*-porphine (TMPyP), a molecule that has been used as a sensitizer for photodynamic cancer therapy,[20] was used for this experiment. The phosphorescence intensity of the probe was monitored as a function of

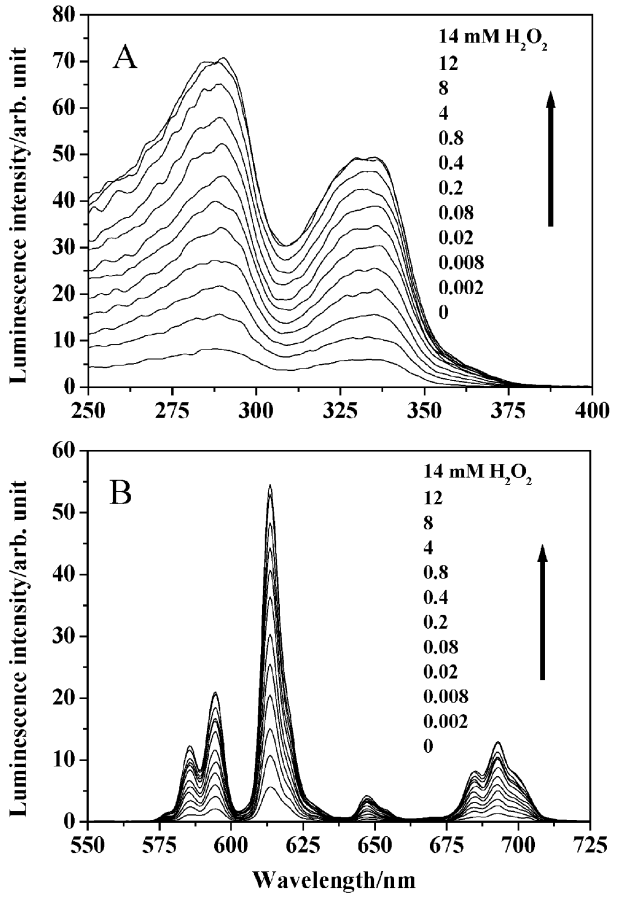

Fig. 4 Time-resolved excitation (A) and emission (B) spectra of ATTA-Eu^{3+} in the reaction with $^1O_2$ generated from the MoO_4^{2-}–H_2O_2 system. A series of H_2O_2 solutions were added to the buffer solutions containing 10 μM of ATTA-Eu^{3+} and 1 mM of Na_2MoO_4. After the reaction, the solutions were diluted 10-fold with 0.05 M borate buffer of pH 9.1, and used for the measurements. The conditions of delay time, 0.2 ms; gate time, 0.4 ms; cycle time, 20 ms; excitation slit, 10 nm; and emission slit, 5 nm were used for the measurements. Excitation spectra were recorded with λ_{em} = 615 nm and emission spectra with λ_{ex} = 335 nm.

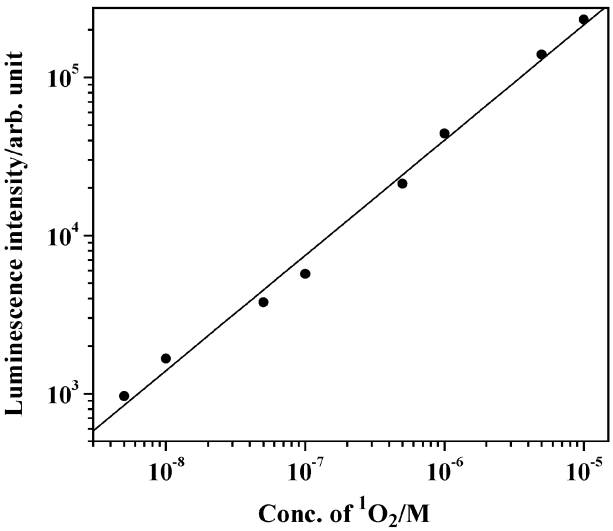

Fig. 5 Calibration curve for $^1O_2$. The curve was derived from the luminescence intensity of the H_2O_2–MoO_4^{2-}–ATTA-Eu^{3+} reaction in 0.1 M carbonate buffer of pH 10.5 with 100 nM of ATTA-Eu^{3+}, 10 mM of Na_2MoO_4 and a series of standard H_2O_2 solutions.

irradiation time. As shown in Fig. 6, the phosphorescence intensity of the probe is distinctly increased with increase in irradiation time, which represents the production of $^1O_2$ during the irradiation, and provides reliable evidence for the ATTA-Eu^{3+} probe for the luminescence detection of $^1O_2$.

The aerobic oxidation of IAA catalyzed by HRP has been studied extensively since 1955.[21] This reaction may provide a molecular basis to explain the action mechanism of IAA as a plant growth regulator. Duran *et al.* and Kanofsky have previously proposed that $^1O_2$ is a product of the aerobic oxidation of IAA catalyzed by HRP at lower pH, but some results are still controversial.[22] In this work, ATTA-Eu^{3+} was successfully used as a phosphorescence probe to monitor the $^1O_2$ generation in such a biochemical system.

First, the effects of various reaction conditions on the $^1O_2$ formation in the IAA–HRP system were investigated using ATTA-Eu^{3+} as a probe. As shown in Fig. 7 and Fig. 8, HRP has a maximal catalytic activity between pH 3 and 4 (which is similar to a reported result[22]), and the amount of $^1O_2$ formed is reduced at both high and low concentrations of HRP. Then the reaction kinetic curves of IAA oxidation catalyzed by HRP were recorded in a 0.05 M sodium acetate buffer of pH 4.0 containing 0.25 μM HRP by monitoring the $^1O_2$ generation with ATTA-Eu^{3+} as a phosphorescence probe. Fig. 9 shows the reaction kinetic curves at different IAA concentrations. The

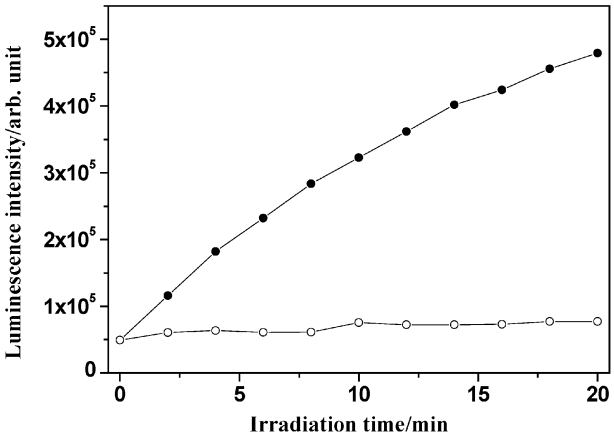

Fig. 6 Reaction of ATTA-Eu^{3+} with $^1O_2$ generated from photosensitization of TMPyP. 100 nM ATTA-Eu^{3+} + 2 μM TMPyP (●) and 100 nM ATTA-Eu^{3+} (○).

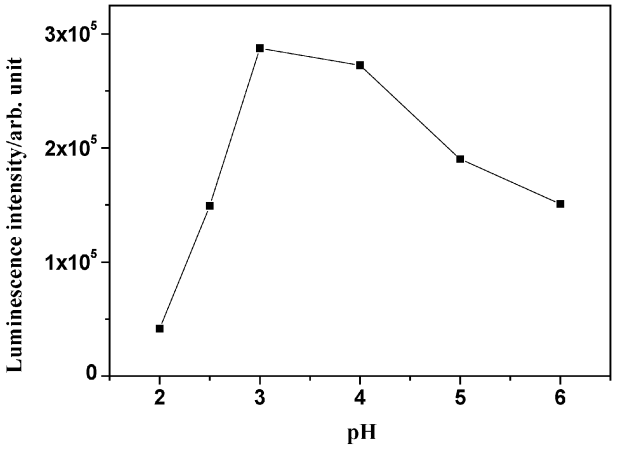

Fig. 7 Effect of pH on the reaction of ATTA-Eu^{3+} with $^1O_2$ generated from the IAA oxidation catalyzed by HRP in a 0.05 M sodium acetate buffer of pH 4.0, containing 100 nM ATTA-Eu^{3+}, 10 μM IAA and 1μM HRP. The luminescence intensities were measured on a Perkin Elmer Victor 1420 Multilabel Counter.

phosphorescence intensity is increased with the augmentation of reaction time from the reaction beginning till reaching a stable value. In the investigated IAA concentration range as shown in Fig. 9, the increase rate of phosphorescence intensity (curve slope) paralleling the formation rate of EP-ATTA-Eu^{3+} is higher at higher concentrations of IAA. To measure the rate constant of EP-ATTA-Eu^{3+} formation in this reaction, we examined the correlation between the concentration of IAA and the initial rate of phosphorescence augmentation. Fig. 10 depicts the dependence of the initial reaction rate on the concentration of IAA, and a good linearity between the two parameters is obtained with a slope of 3.6×10^{-2}, which indicates that the reaction is a first-order reaction related to IAA, and the $^1O_2$ generation in such a biochemical reaction can also be quantitatively detected by using ATTA-Eu^{3+} as a probe. Since the aerobic oxidation of IAA catalyzed by HRP has a very complex process and it is difficult to obtain the rate constant of the $^1O_2$ generation from IAA–HRP system, only the total reaction rate constant (k_{tot}) of the IAA–HRP–ATTA-Eu^{3+} system [eqn. (1), where P is other products than EP-ATTA-Eu^{3+}] was calculated to be 3.6×10^9 M^{-1} S^{-1} from the relationship of reaction rate and concentrations of IAA and ATTA-Eu^{3+}.

$$\text{ATTA} - Eu^{3+} + \text{IAA} \xrightarrow[O_2\text{HRP}]{k_{tot}} \text{EP} - \text{ATTA} - Eu^{3+} + \text{P} \quad (1)$$

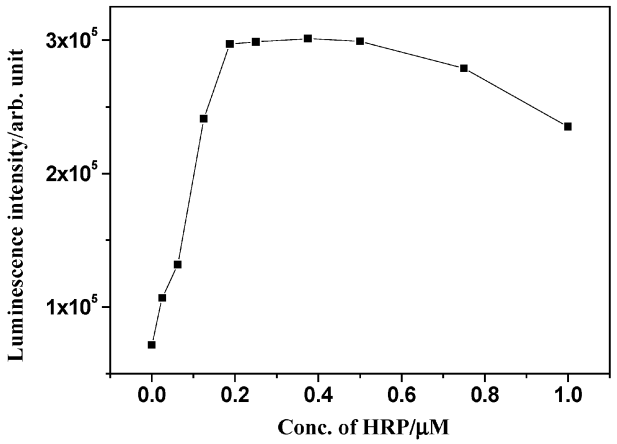

Fig. 8 Effect of HRP concentration on the reaction of ATTA-Eu^{3+} with $^1O_2$ generated from the IAA oxidation catalyzed by HRP in a 0.05 M sodium acetate buffer of pH 4.0, containing 10 μM IAA and 0.1 μM ATTA-Eu^{3+}. The luminescence intensities were measured on a Perkin Elmer Victor 1420 Multilabel Counter.

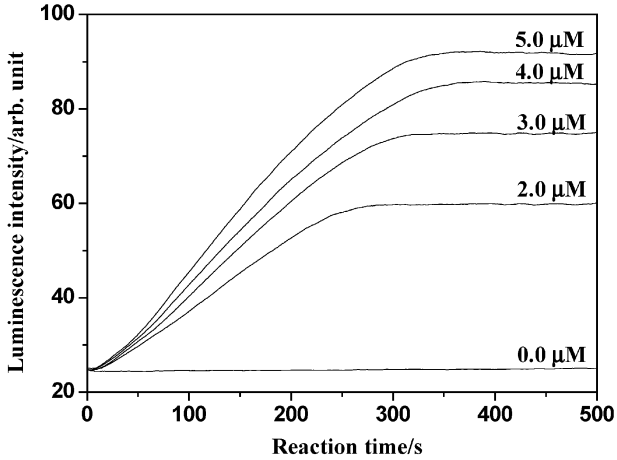

Fig. 9 Reaction kinetic curves of the IAA–HRP–ATTA-Eu^{3+} system (10 μM ATTA-Eu^{3+} and 0.25 μM HRP) at different IAA concentrations. The measurements were carried out on a Perkin Elmer LS 50B luminescence spectrometer with a time-resolved mode and the conditions of delay time, 0.1 ms; gate time, 1.0 ms; cycle time, 20 ms; excitation wavelength, 335 nm; emission wavelength, 615 nm; excitation slit, 10 nm; emission slit, 5 nm; data interval, 1.0 s.

The calibration curve of time-resolved luminescence detection for IAA using the IAA–HRP–ATTA-Eu^{3+} system is shown in Fig. 11. The detection limit, defined as the concentration corresponding to 3 standard deviations of background signal, is 7.8×10^{-8} M. These results indicate that the generation of $^1O_2$ during the aerobic oxidation of IAA catalyzed by HRP at a lower pH can be effectively traced with ATTA-Eu^{3+}.

Detection mechanism consideration of $^1O_2$ with ATTA-Eu^{3+}

The ATTA-Eu^{3+} chelate is the first chemical trap for $^1O_2$ that permits time-resolved luminescence measurement. It reacts with $^1O_2$ to yield its endoperoxide (EP-ATTA-Eu^{3+}), giving sensitive phosphorescence response. Compared with the absorption spectrum of ATTA-Eu^{3+}, the absorption bands of the anthracene moiety are greatly altered after the formation of EP-ATTA-Eu^{3+}, which reveals the unequivocal action of anthracene unit on the probe's trapping ability for $^1O_2$.

The change of the ligand's structure after the reaction of ATTA-Eu^{3+} with $^1O_2$ leads to a great increase in phosphorescence intensity. For a luminescent lanthanide chelate, the overall luminescence quantum yield (ϕ_{tot}) upon exciting the chromophore of the ligand is determined by the efficiency of the sensitization (η_{sens}) and by the quantum yield (ϕ_{Ln}) of the lanthanide luminescence step ($\phi_{tot} = \eta_{sens}\phi_{Ln}$).[23] Because the excited state lifetimes and the chemical environment of the

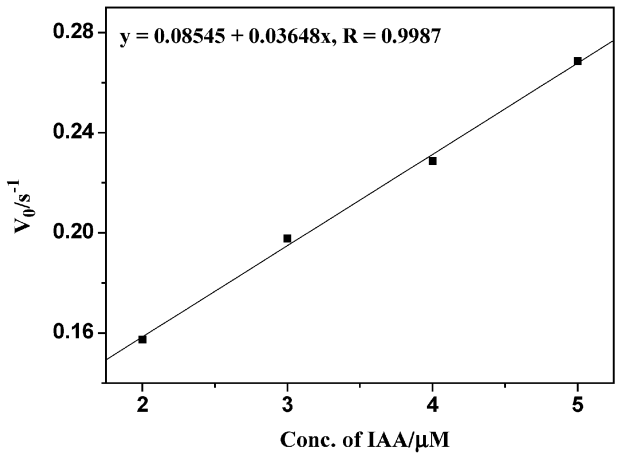

Fig. 10 The plot of initial rates (V_0) of the reaction of IAA–HRP–ATTA-Eu^{3+} against the IAA concentrations.

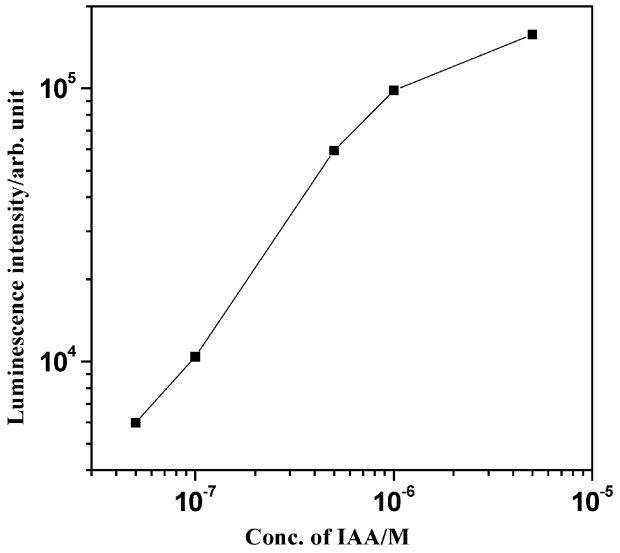

Fig. 11 Calibration curve for IAA. The curve was derived from the luminescence intensity of the IAA–HRP–ATTA-Eu^{3+} reaction in 0.05 M sodium acetate buffer of pH 4.0 with 100 nM of ATTA-Eu^{3+}, 0.25 μM of HRP and a series of standard IAA solutions.

Eu^{3+} ion of the EP-ATTA-Eu^{3+} and ATTA-Eu^{3+} are very similar, the significant increase of luminescence quantum yield can be considered to be due to an increase in the efficiency of the population of the excited state of the Eu^{3+} ion. In the photosensitised luminescence of the Eu^{3+} ion by the ligand, the terpyridine unit acts as a light-absorbing chromophore that serves to photosensitize the Eu^{3+} ion. The excitation of the terpyridine chromophore at 335 nm results in effective population of its triplet level (CT_1, E = 22 400 cm^{-1}), and an intramolecular energy transfer occurs from CT_1 to $^5D_0$ energy level of Eu^{3+} (E = 17 374 cm^{-1}).[13,24] However, the triplet state of anthracene (AT_1, E = 14 900 cm^{-1}) combined with its long lifetime results in a very efficient triplet–triplet quenching, which blocks the effective energy transfer of $CT_1 \rightarrow {}^5D_0$.[25] This accounts for the very weak phosphorescence of ATTA-Eu^{3+}. After the formation of EP-ATTA-Eu^{3+}, the triplet–triplet quenching between CT_1 and AT_1 disappears, thus the Eu^{3+} chelate becomes strongly luminescent.

Conclusion

We have developed a novel Eu^{3+} chelate-based phosphorescence probe specific for time-resolved luminescence detection of $^1O_2$, ATTA-Eu^{3+}, by incorporating a fluorophore of TTA-Eu^{3+} into the anthracene skeleton which can specifically react with $^1O_2$ and efficiently quench the fluorescence of the fluorophore conjugated with it. After ATTA-Eu^{3+} is specifically reacted with $^1O_2$ to yield EP-ATTA-Eu^{3+}, the probe's phosphorescence is strongly enhanced. Compared with the reported organic probes, the properties of high sensitivity, selectivity, kinetic and thermodynamic stability, water solubility and wide pH available range of the new probe for $^1O_2$ detection suggest that the probe should be widely useful for the time-resolved luminescence detection of $^1O_2$ in many chemical and biological systems in aqueous media. The applications of the probe have been exemplified by monitoring the $^1O_2$ generation in an aerobic oxidation system of IAA–HRP and in a photosensitization system of TMPyP. The main drawback of the probe is its lower excitation wavelength, which perhaps makes it not as suitable for some *in vivo* applications. However, the new probe provides a novel strategy for highly sensitive time-resolved luminescence detection of $^1O_2$, which is very useful for some biological systems to eliminate the strong effect of autofluorescence from the samples.

Experimental

Materials and physical measurement

Anhydrous *N*,*N*-dimethylformamide (DMF) was purchased from Acros (Belgium). Tetrahydrofuran (THF) and acetonitrile were used after appropriate distillation and purification. Prior to use, hydrogen peroxide was assayed by using potassium permanganate titration. Horseradish peroxidase (R.Z. 3.0) was purchased from Bio Basic, Inc. Canada. Unless otherwise stated, all chemical materials were purchased from commercial sources and used without further purification.

The ^1H NMR spectra were recorded on a Bruker DRX 400 spectrometer (400 MHz). ESI mass spectra were measured on an Applied Biosystems Mariner System 5303 mass spectrometer. Absorption spectra were measured on a Perkin-Elmer Lambda 35 UV/Vis spectrometer. Elemental analyses were carried out on a Vanio-EL CHN analyser. The time-resolved excitation and emission spectra, and phosphorescence lifetime were measured on a Perkin-Elmer LS 50B luminescence spectrometer (the measurement conditions are given in the figure legends of Fig. 1, 2, 4 and 9). The luminescence quantum yields (ϕ_1) of ATTA-Eu^{3+} and EP-ATTA-Eu^{3+} were measured in a 0.05 M borate buffer of pH 9.1, and calculated by using the equation $\phi_1 = I_1\varepsilon_2C_2\phi_2/I_2\varepsilon_1C_1$ with a standard luminescence quantum yield of ϕ_2 = 0.160 for the Eu^{3+} chelate with 4′-phenyl-2,2′:6′,2″-terpyridine-6,6″-diyl)bis(methylenenitrilo) tetrakis(acetic acid) (molar absorption coefficient $\varepsilon_{335\ nm}$ = 14 300 cm^{-1} M^{-1}).[13] In this equation, I_1 and I_2, ε_1 and ε_2, C_1 and C_2 are the luminescence intensities, molar absorption coefficients, and concentrations for the measured chelate and the standard chelate, respectively. The time-resolved luminescence measurements (Fig. 3, 5–8 and 11) were carried out on a Perkin Elmer Victor 1420 Multilabel Counter with the measurement conditions of excitation wavelength, 340 nm; emission wavelength, 615 nm; delay time, 0.2 ms; window time (counting time), 0.4 ms; and cycling time, 1.0 ms.

Synthesis of (*E*)-3-(9-anthryl)-1-(pyrid-2′-yl) prop-2-enone (1)

After a mixture of 200 ml methanol, 40 ml H_2O, 2.81 g KOH (50 mmol), 10.31 g 9-anthracenecarbaldehyde (50 mmol) and 6.06 g 2-acetylpyridine (50 mmol) was stirred for 24 h at room temperature, the orange precipitate was filtered and recrystallized from ethanol. Compound **1** was obtained (12.77 g, 82.6% yield). ^1H NMR (400 MHz, $CDCl_3$, 25 °C, TMS): δ = 7.48–7.54 (m, 5H; aromatic); 7.92 (m, 1H; aromatic); 8.03 (d, ^3J(H,H) = 8.4 Hz, 2H; aromatic); 8.27–8.31 (m, 2H; aromatic, CH); 8.37 (d, ^3J(H,H) = 8.0 Hz, 2H; aromatic); 8.48 (s, 1H; aromatic); 8.70 (d, ^3J(H,H) = 4.4 Hz, 1H; aromatic); 8.93 (d, ^3J(H,H) = 16.0 Hz, 1H; CH).

Synthesis of 4′-(9-anthryl)-2,2′:6′,2″-terpyridine (2)

A mixture of 15.47 g compound **1** (50 mmol), 23.12 g dry $AcONH_4$ (300 mmol), 16.46 g *N*-[2-(pyrid-2′-yl)-2-oxoethyl] pyridinium iodide (50 mmol), and 500 ml dry methanol was refluxed for 24 h. The solvent was evaporated, and the residue was extracted with 400 ml $CHCl_3$. After evaporation, the residue was purified by silica gel column chromatography using petroleum ether (60–90 °C)–ethyl acetate (2 : 1, v/v) as eluent, and then washed with CH_3CN. Compound **2** was obtained (5.48 g, 26.8% yield). ^1H NMR (400 MHz, $CDCl_3$, 25 °C, TMS): δ = 7.26–7.37 (m, 4H; aromatic); 7.47 (t, ^3J(H,H) = 7.6 Hz, 2H; aromatic); 7.71 (d, ^3J(H,H) = 8.8 Hz, 2H; aromatic); 7.92 (m, 2H; aromatic); 8.07 (d, ^3J(H,H) = 8.8 Hz, 2H; aromatic); 8.55 (s, 1H; aromatic); 8.61 (s, 2H; aromatic); 8.63 (d, ^3J(H,H) = 4.0 Hz, 2H; aromatic), 8.79 (d, ^3J(H,H) = 8.0 Hz, 2H; aromatic). Elemental analysis calcd for $C_{29}H_{19}N_3$: C 85.06, H 4.68, N 10.26; found: C 84.66, H 4.63, N, 9.90%.

Synthesis of 4′-(9-anthryl)-2,2′:6′,2″-terpyridine-6,6″-dicarbonitrile (3)

After a mixture of 160 ml CH_2Cl_2, 6.9 g 3-chloroperbenzoic acid (32.0 mmol), 3.3 g compound **2** (8.0 mmol) was stirred for 24 h at room temperature, the mixture was washed with 10% Na_2CO_3 solution (2 × 150 ml), dried with Na_2SO_4 and evaporated. The residue was dissolved in 200 ml of CH_2Cl_2. To the solution was added 6.34 g Me_3SiCN (64.0 mmol) with stirring. After stirring for 1 h, 5.62 g benzoyl chloride (40.0 mmol) was added dropwise within 20 min, and the solution was stirred at room temperature for 24 h. The solution was evaporated to half of its volume, to the solution was added 200 ml 10% K_2CO_3, and the mixture was further stirred for 1 h. The precipitate was filtered and washed with water and CH_3CN, and dried. Compound **3** was obtained (2.34 g, 63.6% yield). ^{1}H NMR (400 MHz, $CDCl_3$, 25 °C, TMS): δ = 7.40 (t, ^3J(H,H) = 7.2 Hz, 2H; aromatic); 7.50 (t, ^3J(H,H) = 8.0 Hz, 2H; aromatic); 7.63 (d, ^3J(H,H) = 8.8 Hz, 2H; aromatic); 7.75 (d, ^3J(H,H) = 7.2 Hz, 2H; aromatic); 8.05–8.12 (m, 4H; aromatic); 8.61 (s, 1H; aromatic); 8.72 (s, 2H; aromatic); 8.98 (d, ^3J(H,H) = 8.0 Hz, 2H; aromatic).

Synthesis of dimethyl 4′-(9-anthryl)-2,2′:6′,2″-terpyridine-6,6″-dicarboxylate (4)

After a mixture of 12 ml concentrated H_2SO_4, 1.89 g compound **3** (4.1 mmol), 24 ml acetic acid, and 6 ml water was stirred at 90 °C for 12 h, the solution was added to 300 ml ice–water. The precipitate was filtered, washed with water and dried. To 125 ml of cooled methanol (ice–water bath) was added dropwise 4.11 g of thionyl chloride (34.6 mmol). After stirring 30 min at room temperature, the above precipitate was added, and the mixture was refluxed for 24 h. After evaporation, the residue was washed with 10% Na_2CO_3 and purified by silica gel column chromatography using chloroform–methanol (95 : 5, v/v) as eluent. Compound **4** was obtained (1.56 g, 72.4% yield). ^{1}H NMR (400 MHz, $CDCl_3$, 25 °C, TMS): δ = 3.90 (s, 6H; OCH_3); 7.36 (t, ^3J(H,H) = 8.8 Hz, 2H; aromatic); 7.50 (t, ^3J(H,H) = 7.2 Hz, 2H; aromatic); 7.66 (d, ^3J(H,H) = 8.8 Hz, 2H; aromatic); 8.06–8.12 (m, 4H; aromatic); 8.19 (d, ^3J(H,H) = 8.0 Hz, 2H; aromatic); 8.61 (s, 1H; aromatic); 8.73 (s, 2H; aromatic); 8.99 (d, ^3J(H,H) = 7.2 Hz, 2H; aromatic).

Synthesis of 4′-(9-anthryl)-2,2′:6′,2″-terpyridine-6,6″-dimethanol (5)

A mixture of 48 ml dry ethanol, 1.52 g **4** (2.9 mmol) and 0.44 g $NaBH_4$ (11.6 mmol) was stirred for 2 h at room temperature, and further refluxed for 8 h. After the solvent was evaporated, 8 ml of saturated $NaHCO_3$ was added, and the solution was heated to boiling. To the solution was added 60 ml of water, and then the solution was placed in a refrigerator (~4 °C) overnight. The precipitate was filtered and washed with H_2O and CH_3CN. Compound **5** was obtained (1.02 g, 74.9% yield). ^{1}H NMR (400 MHz, $CDCl_3$, 25 °C, TMS): δ = 4.74 (s, 4H, CH_2OH); 7.25 (d, ^3J(H,H) = 7.8 Hz, 2H; aromatic); 7.36 (t, ^3J(H,H) = 7.8 Hz, 2H; aromatic); 7.48 (t, ^3J(H,H) = 7.8 Hz, 2H; aromatic); 7.67 (d, ^3J(H,H) = 8.0 Hz, 2H; aromatic); 7.90 (t, ^3J(H,H) = 7.8 Hz, 2H; aromatic); 8.09 (d, ^3J(H,H) = 8.8 Hz, 2H; aromatic); 8.58 (s, 1H; aromatic); 8.60 (s, 2H; aromatic); 8.68 (d, ^3J(H,H) = 8.0 Hz, 2H; aromatic).

Synthesis of 6,6″-bis(bromomethyl)-4′-(9-anthryl)-2,2′:6′,2″-terpyridine (6)

After a mixture of 40 ml dry DMF and 1.21 g PBr_3 (4.5 mmol) was stirred at room temperature for 15 min, 0.84 g compound **5** (1.8 mmol) was added, and the solution was stirred for 24 h at room temperature. The solution was neutralized to pH 7–8 with saturated $NaHCO_3$, and the precipitate was filtered and washed with water and CH_3CN. Compound **6** was obtained (0.83 g, 77.9% yield). ^{1}H NMR (400 MHz, $CDCl_3$, 25 °C, TMS): δ = 4.52 (s, 4H, CH_2Br); 7.38 (t, ^3J(H,H) = 7.8 Hz, 2H; aromatic); 7.49 (m, 4H; aromatic); 7.70 (d, ^3J(H,H) = 7.8 Hz, 2H; aromatic); 7.92 (t, ^3J(H,H) = 7.8 Hz, 2H; aromatic); 8.10 (d, ^3J(H,H) = 8.0 Hz, 2H; aromatic); 8.59 (s, 1H; aromatic); 8.65 (s, 2H; aromatic); 8.70 (d, ^3J(H,H) = 8.0 Hz, 2H; aromatic).

Synthesis of tetraethyl [4′-(9-anthryl)-2,2′:6′,2″-terpyridine-6,6″-diyl]bis(methylenenitrilo) tetrakis(acetate) (7)

After a mixture of 0.60 g compound **6** (1 mmol), 0.42 g diethyl iminodiacetate (2.2 mmol), 1.38 g dry K_2CO_3 (10 mmol), 70 ml dry CH_3CN and 21 ml dry THF was refluxed for 24 h with stirring, the mixture was filtered. After evaporation, the residue was dissolved in 80 ml $CHCl_3$, and the solution was washed with 80 ml 5% $NaHCO_3$, 80 ml H_2O, and dried with Na_2SO_4. The solvent was evaporated, and the residue was purified by silica gel column chromatography using petroleum ether (60–90 °C)–ethyl acetate–triethylamine (15 : 5 : 2, v/v/v) as eluent. The product was washed with petroleum ether. Compound **7** was obtained (0.55 g, 68.0% yield). ^{1}H NMR (400 MHz, $CDCl_3$, 25 °C, TMS): δ = 1.07 (t, ^3J(H,H) = 7.2 Hz, 12H; CH_3); 3.58 (s, 8H; CH_2); 4.00 (q, ^3J(H,H) = 7.2 Hz, 8H; CH_2); 4.02 (s, 4H; CH_2); 7.37 (t, ^3J(H,H) = 8.0 Hz, 2H; aromatic); 7.48 (t, ^3J(H,H) = 7.2 Hz, 2H; aromatic); 7.64 (d, ^3J(H,H) = 8.0 Hz, 2H; aromatic); 7.72 (d, ^3J(H,H) = 7.2 Hz, 2H; aromatic); 7.90 (t, ^3J(H,H) = 8.0 Hz, 2H; aromatic); 7.72 (d, ^3J(H,H) = 8.0 Hz, 2H; aromatic); 8.57 (s, 3H; aromatic); 7.72 (d, ^3J(H,H) = 8.0 Hz, 2H; aromatic).

Synthesis of ATTA

A mixture of 1.39 g compound **7** (1.7 mmol), 2.02 g KOH (36.0 mmol), 60 ml ethanol and 10 ml H_2O was refluxed for 2 h. After evaporation, the residue was dissolved in 50 ml water, and the solution was filtered. To the solution was added dropwise 1 M HCl to adjust the pH to ~3, and the solution was stirred for 3 h at room temperature. The precipitate was collected by filtration and washed with water. After drying, the product was added to 50 ml of dry acetonitrile, and the mixture was refluxed for 30 min. The precipitate was filtered and dried. ATTA was obtained (0.81 g, 65.6% yield). ^{1}H NMR (400 MHz, DMSO-d_6, 25 °C, TMS): δ = 3.45 (s, 8H; CH_2); 3.96 (s, 4H; CH_2); 7.47 (t, ^3J(H,H) = 8.0 Hz, 2H; aromatic); 7.56–7.63 (m, 4H; aromatic); 7.80(d, ^3J(H,H) = 8.0 Hz, 2H; aromatic); 8.08 (t, ^3J(H,H) = 8.0 Hz, 2H; aromatic); 8.23 (t, ^3J(H,H) = 8.0 Hz, 2H; aromatic); 8.43 (s, 2H; aromatic); 8.69 (d, ^3J(H,H) = 8.0 Hz, 2H; aromatic); 8.82 (s, 1H; aromatic). Elemental analysis calcd for $C_{39}H_{33}N_5O_8 \cdot 1.5H_2O$: C 64.64, H 4.99, N 9.64; found: C 64.52, H 5.38, N 9.30%. ESI-MS: m/z (%): 698 (100) [$M^- - H$].

Synthesis and characterization of endoperoxide of ATTA-Eu^{3+} (EP-ATTA-Eu^{3+})

To 10 ml of 0.1 M carbonate buffer of pH 10.5 were added 36 mg ATTA (0.05 mmol) and 18 mg $EuCl_3 \cdot 6H_2O$ (0.05 mmol). After stirring for 2 h at room temperature, 1.2 g $Na_2MoO_4 \cdot 2H_2O$ (5 mmol) and 500 μl 30% H_2O_2 were added, and the solution was stirred for 30 min. A further 500 μl H_2O_2 was added to the solution, and the reaction was monitored by fluorimetry to check the complete conversion of ATTA-Eu^{3+} to EP-ATTA-Eu^{3+} (part of the solution was used for the measurement of phosphorescence properties). The solution was cooled to 0 °C and acidified to pH ~3 with HCl. The precipitate was centrifuged, washed with water and dried. The product was confirmed by ESI mass spectrum. ESI-MS: m/z

(%): 882 (10) [M^- – H] (unreacted ATTA-Eu^{3+} was not found). Unfortunately we were unable to obtain the precise yield and data of EP-ATTA-Eu^{3+} including ^1H NMR and elemental analysis because of the interference of some inorganic ions abounding in the product. The purification of the endoperoxide is difficult, since the solid endoperoxide is not very stable, which can be reduced by some organic solvents.

Reactions of ATTA-Eu^{3+} with reactive oxygen species

All reactions were carried out in 0.05 M carbonate buffer of pH 10.5 with the same ATTA-Eu^{3+} concentration (100 nM). Superoxide solution was prepared by adding KO_2 to dry dimethyl sulfoxide and stirring vigorously for 10 min.[26] Hydroxyl radical was generated through the Fenton reaction of ferrous ammonium sulfate and hydrogen peroxide.[26] Singlet oxygen was chemically generated from the MoO_4^{2-}–H_2O_2 system in alkaline media.[15]

Detection of $^1O_2$ in aqueous media

The reaction of ATTA-Eu^{3+} with $^1O_2$ generated from a MoO_4^{2-}–H_2O_2 system was performed in 0.1 M carbonate buffer of pH 10.5. A series of H_2O_2 solutions were added to the buffer solutions containing 10 μM of ATTA-Eu^{3+} and 1 mM of Na_2MoO_4. After the reaction, the solutions were diluted 10-fold (final probe concentration = 1.0 μM) with 0.05 M borate buffer of pH 9.1, and the excitation and emission spectra were measured with a time-resolved mode.

The photosensitization reaction was carried out in 0.05 M Tris-HCl buffer of pH 7.4. The buffer solution containing 200 μM TMPyP and 10 μM of ATTA-Eu^{3+} were irradiated from a distance of 2 cm by a 100 W tungsten lamp. After the reaction, the solution was diluted 100-fold (final probe concentration = 100 nM) with the buffer, and the time-resolved luminescence measurement was carried out on a Perkin Elmer Victor 1420 Multilabel Counter.

The experiments of real-time monitoring of $^1O_2$ generation in an HRP-catalyzed oxidation system of IAA were carried out in 0.05 M sodium acetate buffer of pH 4.0. To a series of IAA solutions (2.0 ml) containing 10 μM ATTA-Eu^+ were added 10 μl of 50 μM HRP (the molar concentration of HRP was calculated by using the molecular weight, M_{HRP} = 40 000) under constant stirring. The reaction kinetic curves were recorded simultaneously after the addition of HRP on a Perkin Elmer LS 50B luminescence spectrometer with a time-resolved mode.

Acknowledgements

The authors thank for the partial support from The National Natural Science Foundation of China (20175027) and Scientific Research Innovation Foundation of the Chinese Academy of Sciences.

References

1 (*a*) C. Foote, in *Free Radicals in Biology*, ed. W. A. Pryor, Academic Press, New York, 1976, vol. 2, pp. 85–133; (*b*) H. Sies and C. F. Menck, *Mutat. Res.*, 1992, **275**, 367.
2 (*a*) M. E. Murphy and H. Sies, *Methods Enzymol.*, 1990, **186**, 595; (*b*) J. R. Kanofsky, *Chem. Biol. Interact.*, 1989, **70**, 1.
3 R. D. Scurlock, B. Wang, P. R. Ogilby, J. R. Sheats and R. L. Clough, *J. Am. Chem. Soc.*, 1995, **117**, 10194.
4 (*a*) I. E. Kochevar, M. C. Lynch, S. Zhuang and C. R. Lambert, *Photochem. Photobiol.*, 2000, **72**, 548; (*b*) K. R. Weishaupt, C. J. Gomer and T. J. Dougherty, *Cancer Res.*, 1976, **36**, 2326.
5 (*a*) L. O. Klotz, K. Briviba and H. Sies, *Methods Enzymol.*, 2000, **319**, 130; (*b*) S. W. Ryster and R. M. Tyrrell, *Free Radical Biol. Med.*, 1998, **24**, 1520; (*c*) S. Basu-Modak and R. M. Tyrrell, *Cancer Res.*, 1993, **53**, 4505.
6 (*a*) C. Schweitzer and R. Schmidt, *Chem. Rev.*, 2003, **103**, 1685; (*b*) G. R. Martinez, P. D. Mascio, M. G. Bonini, O. Augusto, K. Briviba, H. Sies, P. Maurer, U. Röthlisberger, S. Herold and W. H. Koppenol, *Proc. Natl. Acad. Sci. USA*, 2000, **97**, 10307.
7 (*a*) A. A. Krasnovsky Jr., *Biol. Membr.*, 1998, **15**, 530; (*b*) T. Keszthelyi, D. Weldon, T. N. Andersen, T. D. Poulsen, K. V. Mikkelsen and P. R. Ogilby, *Photochem. Photobiol.*, 1999, **70**, 531; (*c*) L. K. Andersen, Z. Cao, P. R. Ogilby, L. Poulsen and I. Zebger, *J. Phys. Chem. A*, 2002, **106**, 8488.
8 (*a*) E. J. Corey and W. C. Taylor, *J. Am. Chem. Soc.*, 1964, **86**, 3881; (*b*) H. H. Wasserman, J. R. Scheffer and J. L. Cooper, *J. Am. Chem. Soc.*, 1972, **94**, 4991; (*c*) N. J. Turro, M. F. Chow and J. Rigaudy, *J. Am. Chem. Soc.*, 1981, **103**, 7218; (*d*) M. J. Steinbeck, A. U. Khan and M. J. Karnovsky, *J. Biol. Chem.*, 1992, **267**, 13425; (*e*) M. J. Steinbeck, A. U. Khan and M. J. Karnovsky, *J. Biol. Chem.*, 1993, **268**, 15649.
9 (*a*) N. Umezawa, K. Tanaka, Y. Urano, K. Kikuchi, T. Higuchi and T. Nagano, *Angew. Chem., Int. Ed.*, 1999, **38**, 2899; (*b*) K. Tanaka, T. Miura, N. Umezawa, Y. Urano, K. Kikuchi, T. Higuchi and T. Nagano, *J. Am. Chem. Soc.*, 2001, **123**, 2530.
10 X. H. Li, G. X. Zhang, H. M. Ma, D. Q. Zhang, J. Li and D. B. Zhu, *J. Am. Chem. Soc.*, 2004, **126**, 11543.
11 (*a*) E. Soini and T. Lövgren, *CRC Crit. Rev. Anal. Chem.*, 1987, **18**, 105; (*b*) E. P. Diamandis and T. K. Christopoulos, *Anal. Chem.*, 1990, **62**, 1149A; (*c*) I. Hemmilä and V.-M. Mukkala, *Crit. Rev. Clin. Laboratory Sci.*, 2001, **38**, 441; (*d*) J. Yuan, G. Wang, K. Majima and K. Matsumoto, *Anal. Chem.*, 2001, **73**, 1869.
12 B. Song, G. Wang and J. Yuan, *Chem. Commun.*, 2005, 3553–3555.
13 M. Latva, H. Takallo, V. M. Mukkala, C. Matachescu, J. C. R. Ubis and J. Kankare, *J. Lumin.*, 1997, **75**, 149.
14 (*a*) G. Albano, V. Balzani, E. C. Constable, M. Maestri and D. R. Smith, *Inorg. Chim. Acta*, 1998, **277**, 225; (*b*) G. J. Wilson, A. Launikonis, W. H. F. Sasse and A. W. H. Mau, *J. Phys. Chem. A*, 1997, **101**, 4860.
15 (*a*) J. M. Aubry and B. Cazin, *Inorg. Chem.*, 1988, **27**, 2013; (*b*) J. M. Aubry, B. Cazin and F. Duprat, *J. Org. Chem.*, 1989, **54**, 726.
16 M. H. V. Werts, J. W. Verhoeven and J. W. Hofstraat, *J. Chem. Soc., Perkin Trans. 2*, 2000, 433.
17 A. Beeby, I. M. Clarkson, R. S. Dickins, S. Faulkner, D. Parker, L. Royle, A. S. de Sousa, J. A. G. Williams and M. Woods, *J. Chem. Soc., Perkin Trans. 2*, 1999, 493.
18 O. S. Wolfbeis, A. Dürkpo, M. Wu and Z. Lin, *Angew. Chem., Int. Ed.*, 2002, **41**, 4495.
19 J. R. Harbour and S. L. Issler, *J. Am. Chem. Soc.*, 1982, **104**, 903.
20 A. Villanueva, L. Caggiari, G. Jori and C. Milanesi, *J. Photochem. Photobiol. B: Biol.*, 1994, **23**, 49.
21 R. H. Kenten, *Biochem. J.*, 1955, **59**, 110.
22 (*a*) M. P. De Mello, S. M. De Toledo, M. Haun, G. Cilento and N. Duran, *Biochem.*, 1980, **19**, 5270; (*b*) J. R. Kanofsky, *J. Biol. Chem.*, 1988, **263**, 14171.
23 M. H. V. Werts, R. T. F. Jukes and J. W. Verhoeven, *Phys. Chem. Chem. Phys.*, 2002, **4**, 1542.
24 G. Ofelt, *J. Chem. Phys.*, 1963, **38**, 2171.
25 (*a*) G. Albano, V. Balzani, E. C. Constable, M. Maestri and D. R. Smith, *Inorg. Chim. Acta*, 1998, **277**, 225; (*b*) G. J. Wilson, A. Launikonis, W. H. F. Sasse and A. W. H. Mau, *J. Phys. Chem. A*, 1997, **101**, 4860.
26 H. T. Zhao, S. Kalivendi, H. Zhang, J. Joseph, K. Nithipatikom, J. Vasquez-Vivar and B. Kalyanaraman, *Free Radical Biol. Med.*, 2003, **34**, 1359.